

Formulation and Artificial Sebum Effects on the Percutaneous Absorption of Zinc Pyrithione Through Excised Human Skin

Allison K. Rush^{1**}, J F. Nash², Edward D. Smith III², and Gerald B. Kasting^{1*}

¹ James L. Winkle College of Pharmacy, University of Cincinnati Academic Health Center, Cincinnati, OH, USA

² The Procter & Gamble Company, Cincinnati, OH, USA

* Corresponding Author:

Gerald B. Kasting
James L. Winkle College of Pharmacy
Division of Pharmaceutical Sciences
University of Cincinnati Academic Health Center
3225 Eden Avenue
Cincinnati, OH, 45267, USA
Tel: (513)558-1817
E-mail: Gerald.Kasting@uc.edu

** Present address: arush1@its.jnj.com, Johnson & Johnson Consumer Inc., 199 Grandview Road, Skillman, NJ 08558-9418

Supplementary Material

S1. Review of Zinc Pyrithione (ZnPT) skin penetration data

S1.1 *In vivo percutaneous absorption of ZnPT in laboratory animals*

Studies in multiple animal species show variability in the magnitude of percutaneous absorption for ZnPT (Fig. S1). In these studies, the amount of ZnPT systemically absorbed was determined by measuring a metabolite/degradation product of pyrithione excreted in the urine, the primary route of elimination [1-5]. The data generated by Howes and Black [6] showed that the percutaneous absorption rate of ZnPT deposited onto rat skin from shampoo remained relatively constant as the dose was increased from 12.8 to 230 $\mu\text{g}/\text{cm}^2$. Generally speaking, there is an inverse relationship between applied dose and percent absorption in these studies.

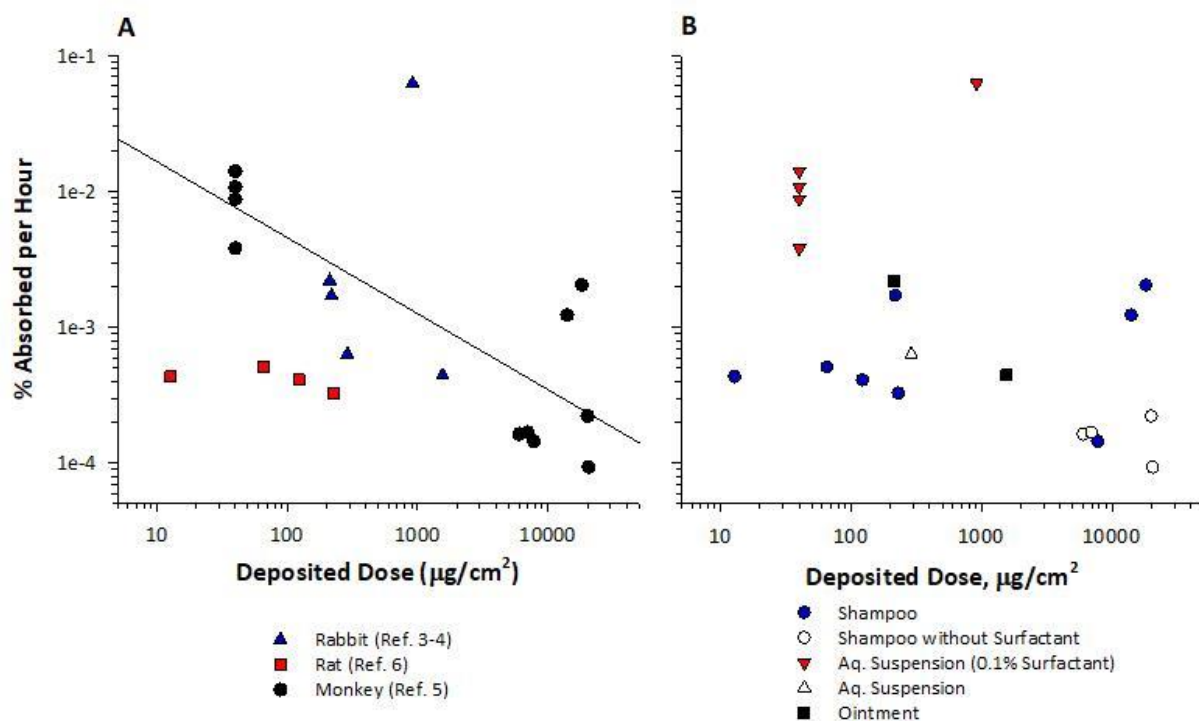


Figure S1. In vivo percutaneous absorption rates of ZnPT deposited (A) on the skin of different animal species and (B) from different formulations using the same data points as Panel A. The amount absorbed is considered to be the amount that was collected in the urine. Linear regression is plotted if the slopes in the dose response curves were significantly less than zero.

S1.2 In vitro human studies

Although animal percutaneous absorption data can be used to estimate the upper limits of absorption in human skin, in vitro human skin studies provide assessments of permeability in the relevant species. A summary from one such study (Study 1 in Table S1) demonstrated this species difference by comparing the in vitro skin permeability of Zn[¹⁴C]PT applied to rat and human skin from an aqueous 1% carboxymethylcellulose solution (CMC) (available in [7]). In the SCCS opinion [7], a 10-fold increase in total absorption of the radioactive dose was observed for rat skin compared to human skin, when total absorption was calculated as the sum of the amount of radioactivity (calculated as µg Zn[¹⁴C]PT-equivalents/cm²) collected in the receptor compartment, viable epidermis and dermis. This 10-fold increase is typical when comparing in vitro skin absorption data for these two species and has been suggested as a correction factor to adjust rat data for use in human dermal risk assessments [8].

The results of in vitro human skin penetration studies with Zn[¹⁴C]PT in hair care formulations (i.e., shampoo or leave-on tonic) or a simple 0.1% surfactant solution are also shown in Table S1 (Study 2 [9] and Study 3 [10]). Taking all of the values from human skin and plotting percent absorption vs. deposited/applied dose (Table S1), an important finding emerges. As shown in Fig. S2 A and B, the skin penetration of radioactivity associated with Zn[¹⁴C]PT was lower when dosed from formulations that did not contain surfactant compared to those that did contain surfactant ($p < 0.01$), which is consistent with present findings (see Table 2). This result may be attributed to the deposited ZnPT being more soluble in

vehicle containing surfactant and, perhaps, in more intimate contact with the skin surface and available to diffuse when dosed from surfactant suspensions.

Table S1. *In vitro* percutaneous absorption of Zn[¹⁴C]PT following a 24 hour collection period. Results are expressed as % of radioactive dose or µg Zn[¹⁴C]PT-equivalents/cm².

Formulation		Dose (µg/cm ²)	Receptor Fluid (%)	Cumulative Absorption	
				Receptor Fluid + Skin (%)	Receptor Fluid + Skin (µg/cm ²)
Study 1 ^a					
Human	1% CMC	101	0.02	0.76 ^b , 1.3 ^c	0.77 ^b , 1.3 ^c
Rat		101	1.1	7.8 ^b , 9.3 ^c	7.9 ^b , 9.3 ^c
Study 2 ^d					
Human	0.1% Surfactant	0.64	19.7	34.4 ^e	0.22
		1.2	10.8	24.4 ^e	0.29
		11.7	3.1	16.5 ^e	1.9
		103	0.37	15.7 ^e	16.2
	1% Shampoo	0.75	8.4	14.7 ^e	0.11
	0.1 % Tonic	5.7	1.1	1.9 ^e	0.11
	0.1% Tonic (No Silicone)	3.3	1.9	3.3 ^e	0.11
	Study 3 ^f				
Human	Dilute Shampoo	0.32	13.6	34.7 ^e	0.11
		0.69	9.9	25.2 ^e	0.17
	Shampoo + Leave-on Tonic	0.87	8.9	23.3 ^e	0.20
		1.7	7.0	18.6 ^e	0.32
	Leave-on Tonic	5.0	0.83	2.5 ^e	0.13
		17.7	0.36	1.2 ^e	0.21
		20.1	0.39	1.2 ^e	0.24
		30.5	0.43	1.2 ^e	0.37
	Shampoo + Leave-on Tonic ^g	4.2	11.3	24.8 ^e	1.0
		7.0	9.3	23.1 ^e	1.6

^a Data publically available in Ref [11]

^b Receptor fluid + viable epidermis + dermis

^c Receptor + viable epidermis + dermis + SC tape strips (6-20)

^d Ref [9]

^e Receptor + epidermis + dermis

^f Ref [10]

^g Repeat administration study (BID for 3 days)

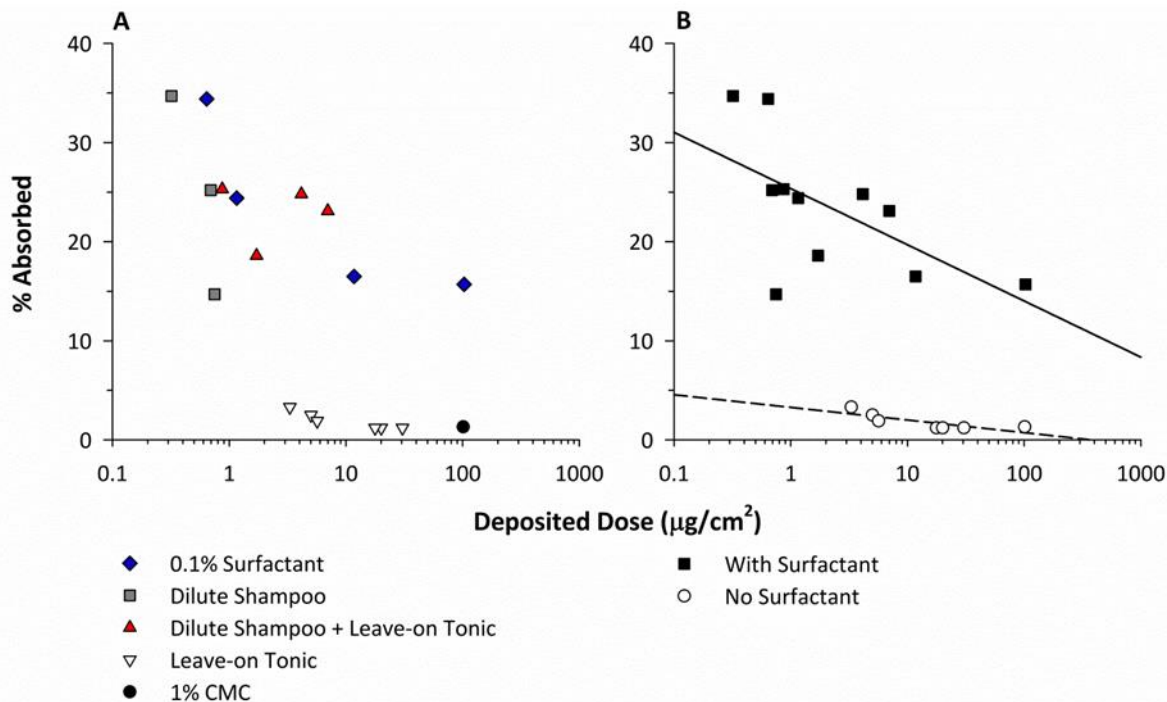


Figure S2. Summary of the Zn[^{14}C]PT in vitro skin penetration data presented in Table S1 for (A) variable formulations (B) with and without surfactant. Non-linear regression is plotted if the slopes in the dose response curves were significantly less than zero.

S1.3. Knowledge gaps in ZnPT skin penetration data

The available data from numerous ZnPT skin penetration studies are difficult to distill into a concise, singular conclusion given the wide range of exposure conditions and lack of replication. Skin dispositions vary between the studies due to intrinsic inter- and intra-species variations in the biophysical characteristics of skin [12] as well as differences in experimental protocols (e.g. vehicles/formulation, dose level, study duration) and subsequent analysis of the data [13-15]. For most compounds, percent absorption is inversely related to mass coverage over a certain dose range and is a relative term that should be interpreted cautiously [16]. Recent analyses have put these relationships on a more quantitative basis [17, 18]. A majority of the ZnPT doses used in the in vivo animal studies and in the cited in vitro human study far exceeded clinically relevant deposition amounts. Considering the low solubility of ZnPT and the fact that only solubilized ZnPT will be absorbed, a majority of these doses remain on the skin surface in crystalline form. Therefore absorption was likely limited by the dissolution rate of ZnPT in the dried product film and/or on the skin surface. In regards to the latter, the process is expected to be slow based on the model-derived [19, 20] value for the amount of ZnPT required to saturate the upper layers of the stratum corneum (SC) barrier ($M_{\text{sat}} = 0.011 \mu\text{g}/\text{cm}^2$). Calculation of this concentration was based on the surface area of the evaporated dose (cm^2) and the following set of equations:

$$M_{\text{sat}} = C_{\text{sat}} \times h_{\text{dep}} \quad (\text{S1})$$

$$C_{\text{sat}} = S_w \times K_{\text{sc/w}} \quad (\text{S2})$$

$$K_{\text{sc/w}} = 0.04 \times K_{\text{o/w}}^{0.81} + 0.0359 + 4.057 \times K_{\text{o/w}}^{0.27} \quad (\text{S3})$$

In Eqs. S1-S3, C_{sat} is the permeant solubility in the SC (g/cm^3), h_{dep} is the initial deposition depth of the permeant (assumed to be 10% of total SC thickness [21] $\sim 1.34 \mu\text{m}$ for partially hydrated SC), S_w is the water solubility of the permeant at skin temperature (32°C), and $K_{sc/w}$ is its SC/water partition coefficient [21, 22]. The concept of a deposition depth is associated with the desquamating layers of the SC and has been useful for describing the skin disposition of small doses of other topically-applied compounds [21, 23, 24].

S2. Results for formulation and sebum effects on the in vitro skin penetration of ZnPT

S2.1. $^3\text{H}_2\text{O}$ skin permeation and Zn[^{14}C]PT dose deposition amounts

$^3\text{H}_2\text{O}$ penetration and Zn[^{14}C]PT deposition amounts are summarized in Figure S3. Significant differences between donors ($p < 0.001$) were observed in the $^3\text{H}_2\text{O}$ flux (Panel A of Fig. S3). Significant differences were also observed in the amount of Zn[^{14}C]PT deposited from the three ZnPT formulations (Panel B of Fig. S3).

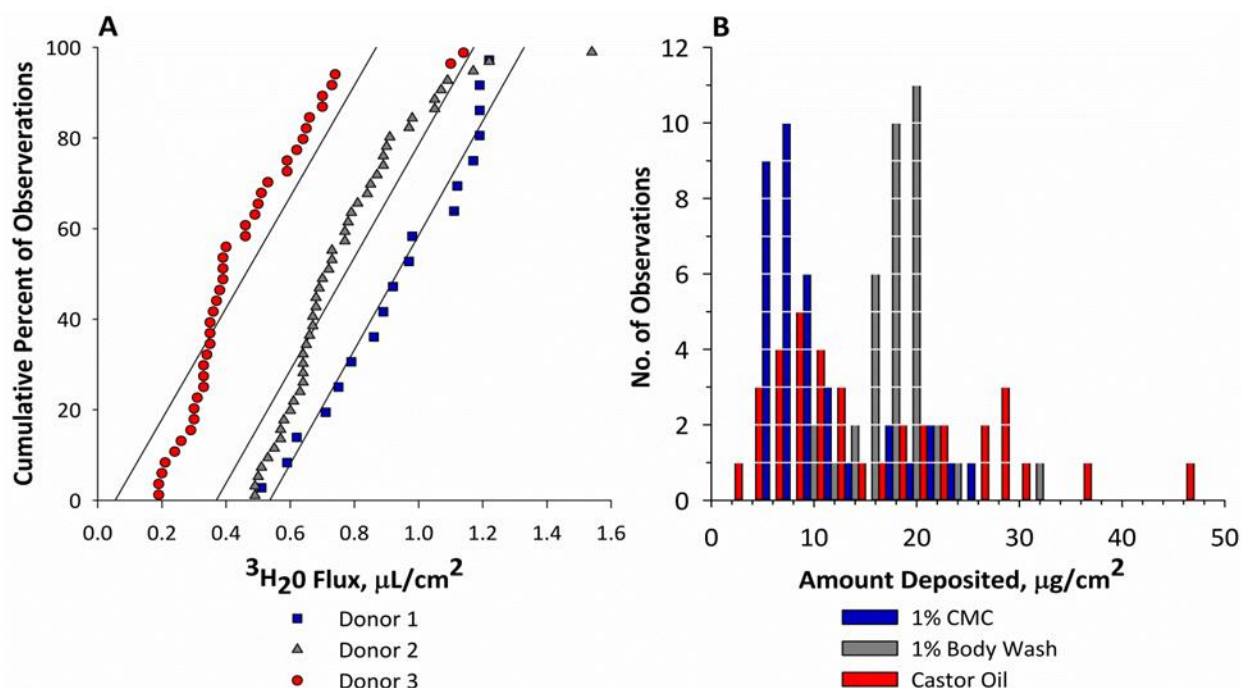


Figure S3. (A) Cumulative distribution of $^3\text{H}_2\text{O}$ permeation for skin samples accepted into each study. (B) Frequency distribution of Zn[^{14}C]PT dose for the three test formulations.

S2.2. Localization of Zn[^{14}C]PT in the excised skin samples

Recovery of radioactivity, expressed as Zn[^{14}C]PT-equivalents, in the various samples is shown in Figure S4. Most of the radioactivity remained on the skin surface and was recovered in the wash samples following a 72-hour exposure period to all six of the topical treatments. In the absence of an artificial sebum layer, less than 3% of the dosed radioactivity penetrated the skin when Zn[^{14}C]PT was applied from the 1% CMC suspension. Under these conditions, the percent of dose penetrated was the highest for the castor oil formulation. Significant differences between formulations ($p < 0.001$) were observed for the wash (i.e. skin surface), epidermis and receptor fluid samples. The presence of the artificial sebum layer did not affect the skin disposition of radioactivity when dosed from the castor oil formulation. However,

significant reductions in the wash amounts were observed for the aqueous suspensions on sebum-supplemented skin compared to untreated skin ($p < 0.001$). Following the deposition of these treatments, more of the compound penetrated into the viable epidermis ($p < 0.001$ for 1% CMC, $p < 0.01$ for 1% body wash) or permeated into the receptor fluid ($p < 0.001$).

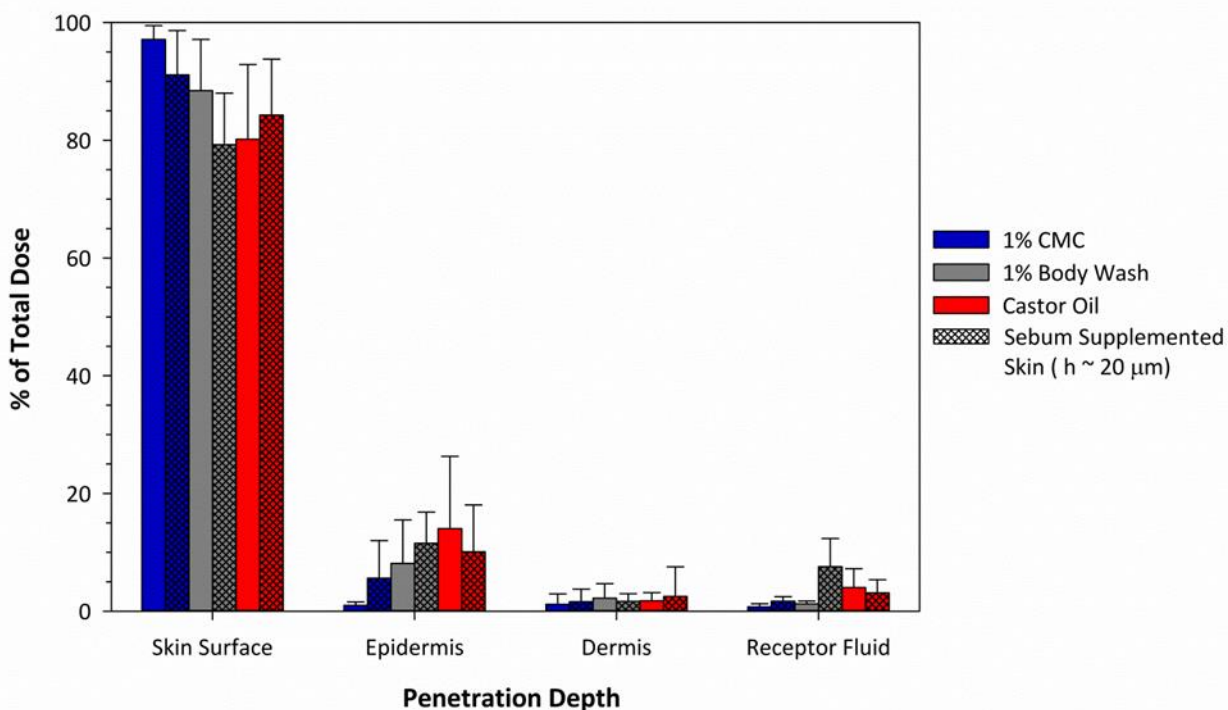


Figure S4. Skin disposition of radioactivity associated with Zn[¹⁴C]PT for the three test formulations in the presence (cross-bar) and absence of an artificial sebum film (h ~ 20 μm).

S3. Model-derived diffusivities of hypothetical pyrrhione moieties

Molecular transformations of ZnPT would modify the physicochemical properties, solubility, and successive mass transport rates of the carbon-14 labeled pyrrhione species (Table S2). It is likely that these transformations explain the treatment effects on percutaneous absorption that were measured in this study. While no experimental data is available regarding the speciation of ZnPT, solubility data using LCMS and ICP to detect pyrrhione or zinc concentrations, respectively, can be compared among the formulations used in the present study. These analyses revealed reductions in the pyrrhione to zinc ratio when ZnPT was solubilized in castor oil (1.6:1) or the artificial sebum composition (0.43-0.9:1) compared to water (2.2:1). These ratios indicate an increase in the concentration of solubilized pyrrhione species containing zinc. The predominant pyrrhione species that are present within the stable pH range in water are the 1:1 ZnPT⁺ monomer and ionized pyrrhione, each accounting for approximately 40-50% of the total pyrrhione concentration¹. We surmise that coordinate covalent bonding between the 1:1 ZnPT⁺ monomer and anions in the formulation or on the skin surface is probable. Theoretical structures were proposed in [25] for the complexation of the 1:1 ZnPT⁺ monomer species to the anionic sodium lauryl sulfate surfactant (ZnPT-SLS) present in the body wash or the deprotonated oleic acid (ZnPT-OA) in the artificial sebum composition. Compared to the intact 1:2 ZnPT monomer, these ligand exchange products

¹ Personal communication Prof Silvio Sammartano University of Messina.

would enhance the solubility of the zinc chelate and help to explain the decreases in the pyrithione to zinc ratios. When oleic acid was removed from artificial sebum composition, the pyrithione to zinc ratio was increased to 1.5:1 (E.D. Smith and J.M. Heinrich, personal communication). Furthermore, a significant ($p < 0.001$) increase was measured for the solubility of Zn^{14}C PT in the artificial sebum comprised of oleic acid and olive oil (95 ± 18 PPM) compared to olive oil only (27 ± 1 PPM). This fluctuation in the pyrithione to zinc ratio along with increased total solubility suggests that the oleic acid is involved in the dissolution of the zinc complex, potentially through a ligand exchange mechanism.

Simulations using the Wang et al. model [19, 20] illustrate the variability in the predicted absorption of the various pyrithione species over time (Fig. S5). The calculated curves that are presented in Fig. S5 are for doses that are stoichiometrically equivalent to $13.8 \mu\text{g}/\text{cm}^2$ ZnPT, the average amount deposited in the in vitro skin penetration study results presented in the main text. According to the model-derived values [19, 20], only the free pyrithione, dipyrithione, and ZnPT^+ complex ion species have M_{sat} values above the doses deposited in this study to enable diffusion-limited permeation. Conversely, the lower permeation and higher lag times of the other pyrithione species is likely attributable to dissolution rate-limited permeation. Although the high lipophilicity of the ligand exchange products, i.e., ZnPT-SLS, ZnPT-OA, could potentially enhance partitioning into the SC barrier, the sizes of these complexes are larger than SC lipid molecules (MW ~ 400 Da); therefore permeation kinetics would likely be limited by the lateral diffusivity of the lipids around which the solutes are intercalated [43]. Comparison of the relatively large ZnPT ligand exchange products demonstrates the dependence of the aliphatic chain size and configuration on permeation. The linear, C12 chain ZnPT complex with sodium lauryl sulfate (ZnPT-SLS) was predicted to penetrate faster and to a greater extent than ZnPT₂ and the branched, C18 chain ZnPT complex with oleic acid (ZnPT-OA).

Table S2. Physicochemical properties and model-derived [37,38] transverse diffusivities of the probable diffusing pyrithione species.

Molecular Species	MW	a_s^b , Å	Log $K_{o/w}^a$	mp ^g , °C	M_{sat}^c , μg/cm ²	D_{\perp} (calc) ^d x 10 ¹² , cm ² s ⁻¹
ZnPT ₂	317.7	5.1	0.97 ^f	240	0.0011	1.1
ZnPT ⁺	192.6	2.7	-1.33 ^g	78	130	0.56
Pyrithione (HPT) ^e	127.2	2.7	-0.30 ^g	25	100	5.1
Dipyrithione (PT ₂)	252.3	4.0	0.60 ^h	191	12	1.6
ZnPT-SLS	456.9	5.9	7.23 ^g	262	0.0041	5.7
ZnPT-OA	473.0	6.4	8.43 ^g	260	0.0011	3.6

^a Octanol/water partition coefficient

^b Estimated hydrodynamic radius

^c Equation 4.1

^d Ref [19, 20]

^e Predominant pyrithione tautomer [26]

^f Ref [11]

^g Ref [27]

^h Ref [28]

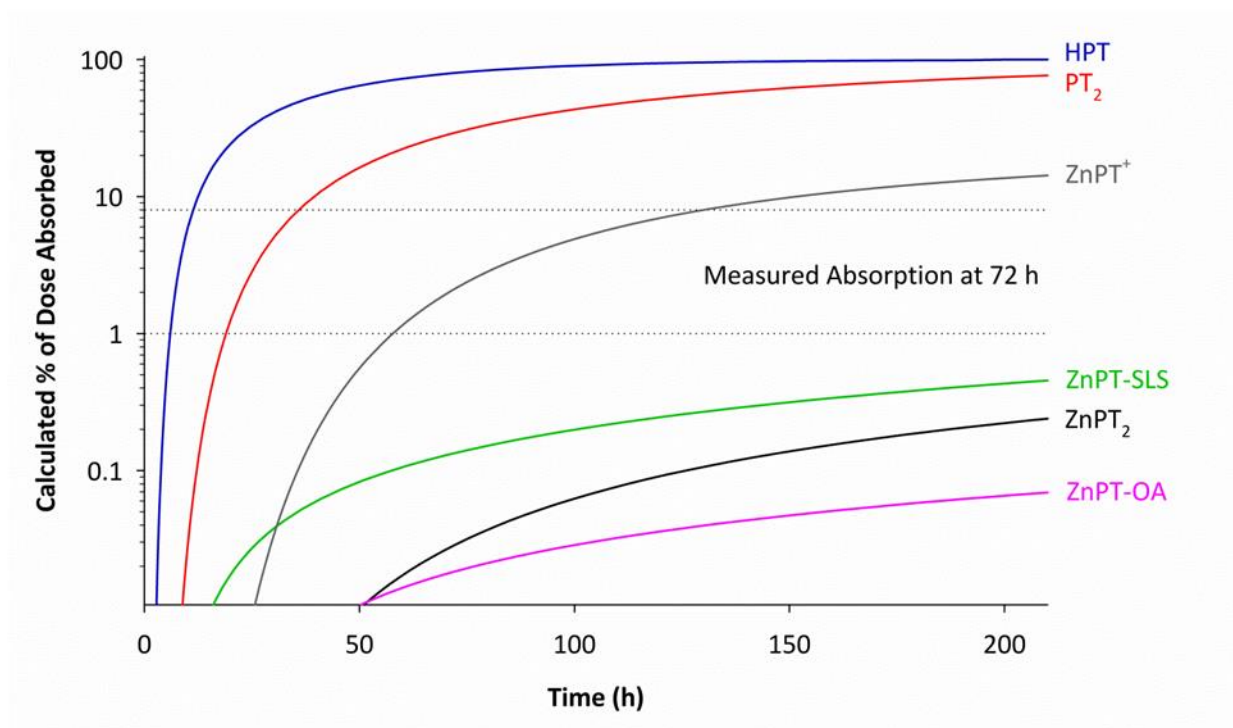


Figure S5. Simulated percutaneous absorption of the various pyrithione species as a function of time for a $13.8 \mu\text{g}/\text{cm}^2$ ZnPT dose. Absorption values between 1-8% are bracketed to display the percent absorption measured in this study after 72 hours of dermal exposures to the various treatments.

References

- 1 Ziller SA: Absorption, excretion and tissue distribution of 2-pyridinethiol-1-oxide. *Food Cosmet Toxicol* 1977;15:49-54.
- 2 Jeffcoat AR, Gibson WB, Rodriguez PA, Turan TS, Hughes PF, Twine ME: Zinc pyridinethione: urinary metabolites of zinc pyridinethione in rabbits, rats, monkeys, and dogs after oral dosing. *Toxicol Appl Pharmacol* 1980;56:141-154.
- 3 Klaassen CD: Absorption, distribution, and excretion of zinc pyridinethione in rabbits. *Toxicol Appl Pharmacol* 1976;35:581-587.
- 4 Okamoto K, Ito T, Hasegawa A, Urakubo G: Percutaneous absorption and residual amount on skin surface of zinc bis(2-pyridylthio)-1,1'-dioxide. *Eisei Kagaku* [translated] 1967;13:323-329.
- 5 Gibson WB, Calvin G: Percutaneous absorption of zinc pyridinethione in monkeys. *Toxicol Appl Pharmacol* 1978;43:425-437.
- 6 Howes D, Black JG: Comparative percutaneous absorption of pyrrithiones. *Toxicol* 1975;5:209-220.
- 7 SCCS_(Scientific_Committee_on_Consumer_Safety): Opinion on Zinc Pyrithione 2013,
- 8 van Ravenzwaay B, Leibold E: A comparison between in vitro rat and human and in vivo rat skin absorption studies. *Hum Exp Toxicol* 2004;23:421-430.
- 9 In_Vitro_Technologies_Inc.(Testing_Facility): In vitro percutaneous absorption and cutaneous disposition of [¹⁴C]zinc pyrithione across intact human skin: Internal P&G Report (Study # M-050499-01), P&G (Sponsor), 1999.
- 10 In_Vitro_Technologies_Inc.(Testing_Facility): In vitro percutaneous absorption and cutaneous disposition of [¹⁴C]zinc pyrithione across intact human skin: Internal P&G Report (Study # M-101199-01), P&G (Sponsor), 2002.
- 11 SCCS_(Scientific_Committee_on_Consumer_Safety): Opinion on Zinc Pyrithione COLIPA n° P81, 2013.
- 12 Couturaud V: Biophysical characteristics of the skin: relation to race, sex, age, and site; in Barel AO, Paye M, Maibach HI (eds): *Handbook of Cosmetic Science and Technology*. Boca Raton, CRC Press, 2014, pp 3-18.
- 13 Henning A, Schaefer UF, Neumann D: Potential pitfalls in skin permeation experiments: influence of experimental factors and subsequent data evaluation. *Eur J Pharm Biopharm* 2009;72:324-331.
- 14 Kasting GB, Filloon TG, Francis WR, Meredith MP: Improving the sensitivity of in vitro skin penetration experiments. *Pharm Res* 1994;11:1747-1754.
- 15 van de Sandt JJ, van Burgsteden JA, Cage S, Carmichael PL, Dick I, Kenyon S, Korinth G, Larese F, Limasset JC, Maas WJ, Montomoli L, Nielsen JB, Payan JP, Robinson E, Sartorelli P, Schaller KH, Wilkinson SC, Williams FM: In vitro predictions of skin absorption of caffeine, testosterone, and benzoic acid: A multi-centre comparison study. *Regul Toxicol Pharmacol* 2004;39:271-281.
- 16 Wester RC, Maibach HI: Relationship of topical dose and percutaneous absorption in rhesus monkey and man. *J Invest Dermatol* 1976;67:518-520.
- 17 Frasch HF, Dotson GS, Bunge AL, Chen C-P, Cherrie JW, Kasting GB, Kissel JC, Sahmel J, Semple S, Wilkinson S: Analysis of finite dose dermal absorption data: Implications for dermal exposure assessment. *J Expos Sci Environ Epidemiol* 2014;24:65-73.
- 18 Kissel JC, Bunge AL, Frasch HF, Kasting GB: Dermal exposure and absorption of chemicals; in McQueen C (ed) *Comprehensive Toxicology*. New York, Elsevier Science, 2017
- 19 Wang TF, Kasting GB, Nitsche JM: A multiphase microscopic diffusion model for stratum corneum permeability. I. Formulation, solution, and illustrative results for representative compounds. *J Pharm Sci* 2006;95:620-648.

- 20 Wang T-F, Kasting GB, Nitsche JM: A multiphase microscopic diffusion model for stratum corneum permeability. II. Estimation of physicochemical parameters, and application to a large permeability database. *J Pharm Sci* 2007;96:3024-3051.
- 21 Kasting GB, Miller MA: Kinetics of finite dose absorption through skin 2. Volatile compounds. *J Pharm Sci* 2006;95:268-280.
- 22 Nitsche JM, Wang T-F, Kasting GB: A two-phase analysis of solute partitioning into the stratum corneum. *J Pharm Sci* 2006;95:649-666.
- 23 Miller MA, Kasting GB: Towards a better understanding of pesticide dermal absorption: diffusion model analysis of parathion absorption in vitro and in vivo. *J Toxicol Environ Health* 2010;73:284-300.
- 24 Gajjar RM, Miller MA, Kasting GB: Evaporation of volatile organic compounds from human skin in vitro. *Ann Occup Hyg* 2013;57:853-865.
- 25 Rush AK: Improving the mechanistic understanding of zinc pyrithione bioavailability in skin through lateral and transverse diffusion measurements: Pharmaceutical Sciences, University of Cincinnati, 2015, PhD.
- 26 Bond A, Jones W: 1-Hydroxy-2(1H)-pyridinethione. *Acta Crystallograph* 1999;C55:1536-1538.
- 27 US_EPA: Estimation Programs Interface Suite™ for Microsoft® Windows. Washington, DC, USA, United States Environmental Protection Agency, 2009,
- 28 NIH: National Center for Biotechnology Information: PubChem Compound Database. . Bethesda, MD, NIH, 2015, 2015.